Quantitative Determination of Intermolecular Interactions with Fluorinated Aromatic Rings

Harry Adams,[a] Jose-Luis Jimenez Blanco,[a] Gianni Chessari,[a] Christopher A. Hunter,*[a] Caroline M. R. Low,[b] John M. Sanderson,[a] and Jeremy G. Vinter[b]

Abstract: The chemical double mutant cycle approach has been used to investigate substituent effects on intermolecular interactions between aromatic rings and pentafluorophenyl π-systems. The complexes have been characterised using ^{1}H and ^{19}F NMR titrations, X-ray crystal structures of model compounds and molecular mechanics calculations. In the molecular zipper system used for these experiments, H-bonds and the geometries of the interacting surfaces favour the approach of the edge of the aromatic ring with the face of the pentafluorophenyl π-system. The interactions are generally repulsive and this repulsion increases with more electron-withdrawing substituents up to a limit of $+2.2$ kJ mol^{-1}, when the complex distorts to minimise the unfavourable interaction. Strongly electron-donating groups cause a change in the geometry of the aromatic interaction and attractive stacking interactions are found (-1.6 kJ mol^{-1} for NMe_2). These results are generally consistent with an electrostatic model: the polarisation of the pentafluorophenyl ring leads to a partial positive charge located at the centre and this leads to repulsive interactions with the positive charges on the protons on the edge of the aromatic ring; when the aromatic ring has a high π-electron density there is a large electrostatic driving force in favour of the stacked geometry which places this π-electron density over the centre of the positive charge on the pentafluorophenyl group.

Keywords: aromaticity · computer chemistry · noncovalent interactions

Introduction

Noncovalent interactions between aromatic motifs influence and control many natural self-assembly and molecular recognition processes, which are responsible for the formation of the double helix of DNA and the tertiary structures of proteins.[1–4] Experimental and theoretical studies suggest that the aromatic interaction is mainly driven by electrostatic and dispersion forces.[5–8] In particular, the interactions between quadrupole moments (Q) arising from the aromatic π-clouds play a fundamental role.[9] It is possible to change the magnitude of the aromatic interaction by introducing substituents on the aromatic motif, which are able to change the quadrupole moment.[7] Of particular interest is the hexafluorobenzene (C_6F_6) molecule, in which all the six protons of the benzene (C_6H_6) are substituted by six electronegative fluorine atoms. This change reverses the quadrupole moment of the molecule (see Figure 1).

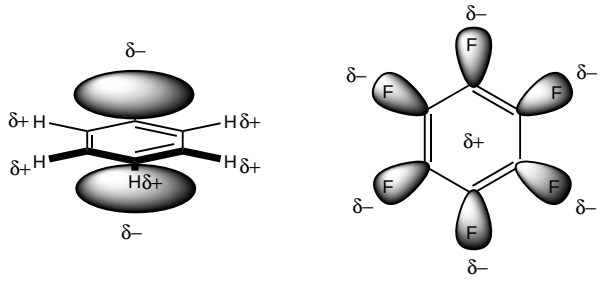

Figure 1. Representation of the charge distribution on hexafluorobenzene (a) and benzene (b).

C_6H_6 and C_6F_6 have molecular quadrupole moments that are similar in magnitude, yet opposite in sign ($Q_{C6H6} = -29.0 \times 10^{-40}$ and $Q_{C6F6} = 31.7 \times 10^{-40}$ C m^{-2}).[10] Therefore, the face-to-face stacks of alternate molecules of C_6H_6 and C_6F_6 observed in the solid state can be explained on the basis of minimisation of quadrupole–quadrupole interaction energies.[11–13] Further support for the importance of electro-

[a] Prof. C. A. Hunter, H. Adams, Dr. J.-L. Jimenez Blanco, Dr. G. Chessari, Dr. J. M. Sanderson
Centre for Chemical Biology
Krebs Institute for Biomolecular Science
Department of Chemistry, University of Sheffield
Sheffield, S37HF (UK)
Fax: (+44) 144-2738673
E-mail: c.hunter@shef.ac.uk

[b] Dr. C. M. R. Low, Dr. J. G. Vinter
James Black Foundation
68 Half Moon Lane, Dulwich, London, SE24 9JE (UK)

0947-6539/01/0716-3494 $ 17.50+.50/0

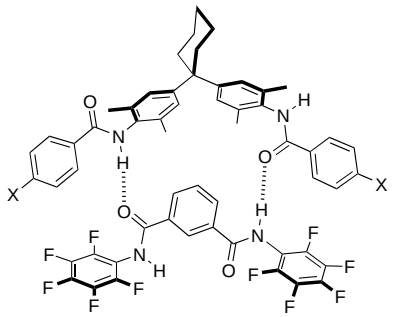

Scheme 1. Complex that could be used to measure the pentafluorophenyl aryl interaction using the double mutant cycle approach (X = NMe_2, *t*Bu, H, F, I, CF_3, NO_2).

statics in such interactions comes from elegant studies of rotational barriers in 1,8-diarylnaphthalenes derivatives and from theoretical studies on metal complexes.[14, 15] The pentafluorophenyl–phenyl interaction has been used to control crystal structure architectures of diynes, olefins and diolefins for photoreactions in the solid state.[16, 17] Also, fluorination of aromatic rings can have a dramatic effect on the interaction of a substrate with a biological receptor.[9] In this work, we apply the chemical double mutant cycle methodology previously described to quantify the pentafluorophenyl–phenyl interaction and to study the effect of phenyl substituents on the magnitude of the interaction.[18]

Approach: The pentafluorophenyl–aryl interaction could potentially be measured by performing mutations on the complex shown in Scheme 1. Initial attempts using the bispentafluorophenyl isophthalamide proved difficult however due to low solubility in $CHCl_3$. Therefore, the unsymmetrical complex, **A** in Scheme 2, was chosen and a double mutant cycle was designed (Scheme 2). The difference in free energy observed on mutating complex **A** into complex **B** ($\Delta G_A - \Delta G_B$) is related to the magnitude of the terminal pentafluorophenyl–aryl interaction in complex **A**. However, the strengths of other secondary interactions are also changed by this mutation and their magnitude can be estimated by mutating complex **C** to complex **D**. Therefore, it is possible to dissect out the pentafluorophenyl–aryl interaction in complex **A** from all the other contributions [Eq. (1)].

$$\Delta\Delta G_{exp} = (\Delta G_A - \Delta G_B) - (\Delta G_C - \Delta G_D) = \Delta G_A - \Delta G_B - \Delta G_C + \Delta G_D \quad (1)$$

It is possible to quantify the free energies directly by measuring the binding constants of the complexes using ^{1}H NMR titrations. The method is based on two important assumptions.

1) The entropy differences between the complexes in Scheme 2 are cancelled out by the double mutant cycle; therefore $\Delta\Delta G$ is equivalent to the enthalpy.
2) Desolvation effects in $CHCl_3$ are small and are qualitatively similar for all substituents X.

Using this approach, the magnitude of the pentafluorophenyl–aryl interaction in $CHCl_3$ for a series of substituents (X = NMe_2, *tert*-butyl, H, F, I, CF_3 and NO_2) was determined.

Results and Discussion

Model compounds: The complexes in Scheme 2 have relatively low binding constants and consequently obtaining good crystals for X-ray studies has not been possible. Therefore, in order to probe the geometry of the aromatic interaction under investigation in complex **A**, we used model compounds **12**–**14**. Amides **12**–**14** were prepared using standard amide coupling reactions between *para*-substituted benzoyl chlorides and pentafluoroaniline (Scheme 3). Crystals of suitable quality for X-ray crystal structure determinations were grown and the structures were solved. In the solid state, the molecules are arranged in infinite H-bonded chains as was previously observed for the model compound **17** (Figure 2a). In **17**, the presence of isopropyl groups constrains the aromatic rings to an edge-to-face geometry. In the model compounds **12**–**14**, less bulky fluorine atoms replace the isopropyl groups, and as a consequence, the aromatic rings have more rotational freedom. Therefore, while the presence of nitro and dimethylamino

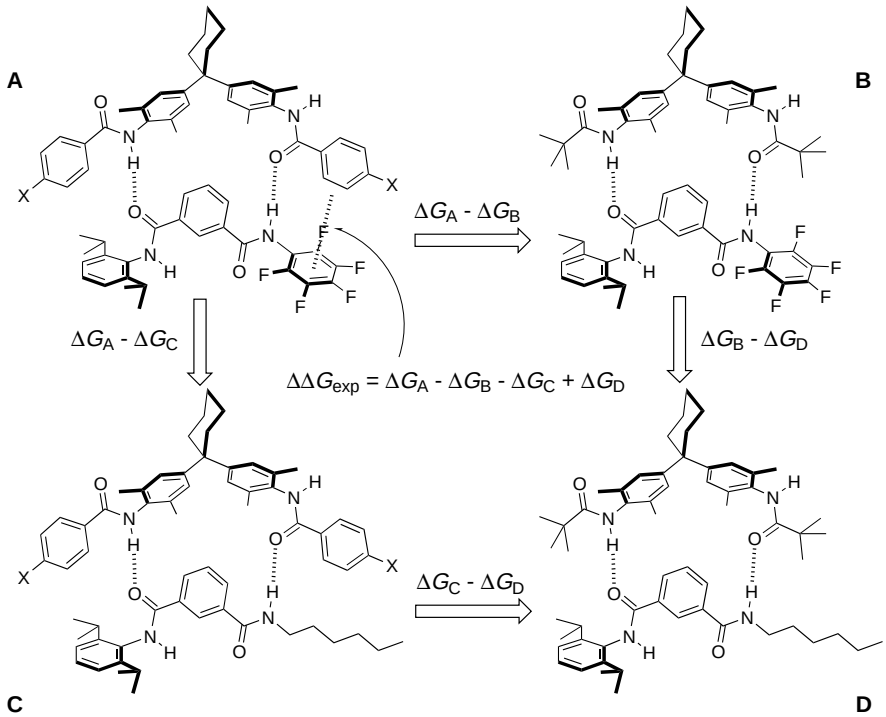

Scheme 2. Differences in free energy observed on mutating complexes (X = NMe_2, *t*Bu, H, F, I, CF_3, NO_2).

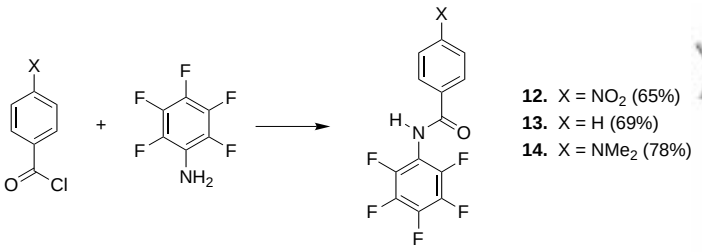

12. X = NO_2 (65%)
13. X = H (69%)
14. X = NMe_2 (78%)

Scheme 3. Preparation of amides **12**–**14** using standard amide coupling reactions between *para*-substituted benzoyl chlorides and pentafluoroaniline.

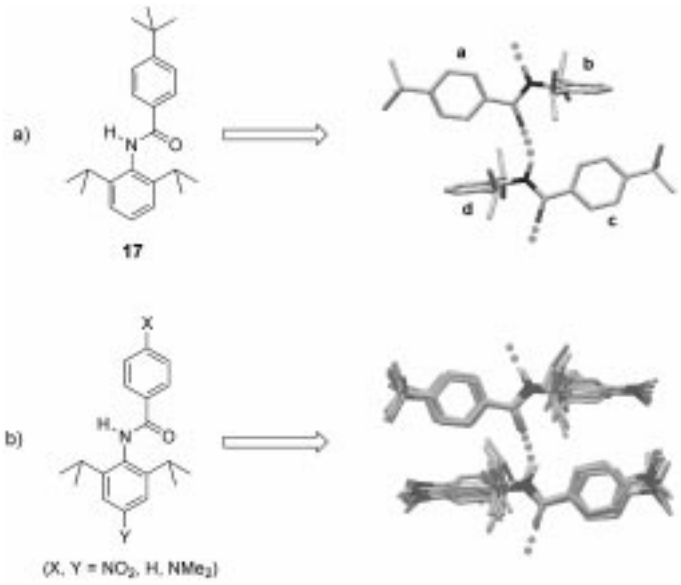

Figure 2. a) Model compound **17** and part of the X-ray crystal structure; b) Overlay of dimers found in the solid state of model compounds; the overlay shows that the substituents NO_2, H and NMe_2 do not significantly alter the geometry of the dimer in **A** for 2,6-diisopropyl aniline derivatives.

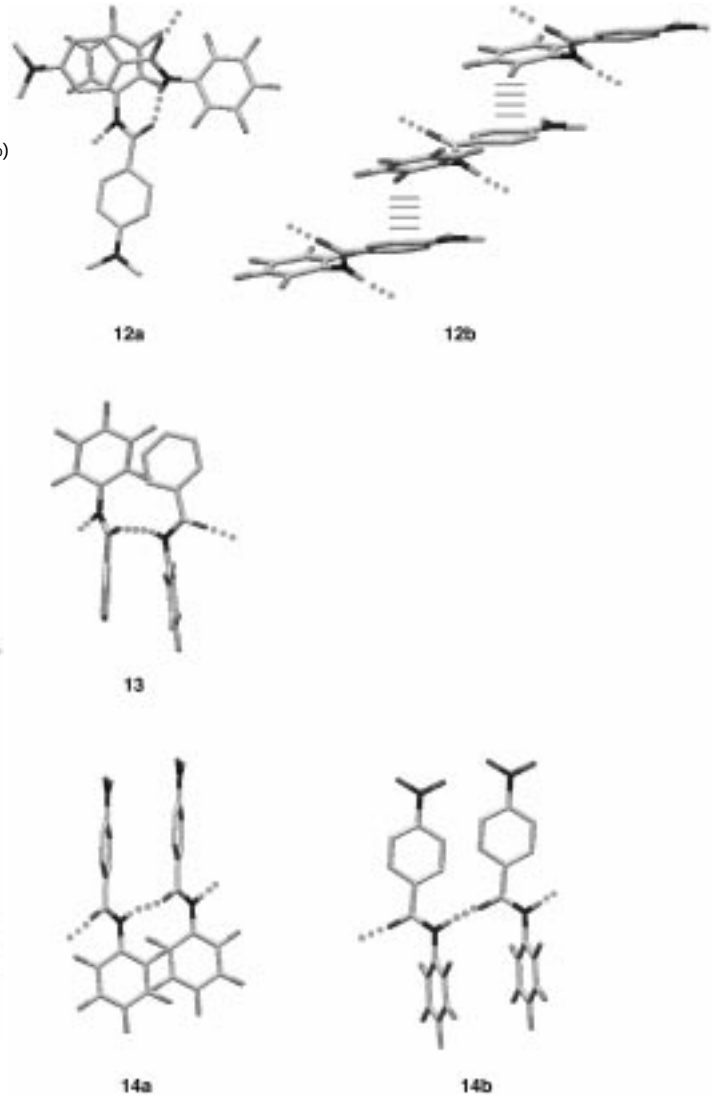

Figure 3. Dimer complexes found in the X-ray crystal structures of model compounds **12**–**14**.

substituents in **17** did not essentially alter the geometry of the 2,6-diisopropyl dimers in Figure 2b,[19] the structure of the pentafluorophenyl dimers **12**–**14** changes dramatically with substituents (Figure 3). When the substituent is NMe_2, pentafluoro–phenyl stacking interactions are observed between hydrogen-bonded dimers (**12a**) and between hydrogen-bonded chains (**12b**). When the *para*-substituent is hydrogen (**13**), offset phenyl–pentafluorophenyl stacking interactions are present. Finally, when NO_2 is present, no interactions are observed between the pentafluorophenyl and aryl rings (**14a**,**b**). Instead offset phenyl–phenyl and pentafluorophenyl–pentafluorophenyl stacking interactions are preferred.

The melting points of the crystals also depend strongly on the substituent: 155 °C (X = NO_2), 184 °C (X = H) and 244 °C (X = NMe_2). This supports the structural evidence that the aryl-pentafluorophenyl stacking interaction in **12** is the strongest, followed by the aryl–pentafluorophenyl offset stacking interaction in **13** and the aryl–aryl/pentafluorophenyl–pentafluorophenyl offset stacking interactions in **14**. The nitro aryl–pentafluorophenyl interaction is not observed, presumably because it is energetically unfavourable.

Double mutant cycles: All the compounds used in the double mutant cycles in Scheme 2 were prepared in reasonable yield by amide coupling reactions using well-established procedures. The structures and syntheses of compounds **1**, **6**, **7** and **8** are described in Schemes 4, 5 and 6 as well as in the Experimental Section. Compounds **3**, **4**, **5**, **9**, **10**, **11**, **15** and **16** have been previously described.[20, 21] The binding constants (K_a) of the complexes were measured by ^{1}H NMR titrations in $CHCl_3$ at room temperature (295 K). For each complex, the K_a values and the binding free energies (ΔG) are reported in Table 1 and the limiting complexation-induced changes in chemical shift ($\Delta\delta$) are in Tables 2 and 3.

All the amide NHs are characterised by large positive $\Delta\delta$ values and this is indicative of H-bonding. In complex **A**, the $\Delta\delta$ values for **nh1** are always larger than the corresponding $\Delta\delta$ values for **nh2**. As a result of the low symmetry of the isophthaloyl compound, which has *trans* oriented amides, these complexes can adopt two different conformations, which are illustrated in Scheme 7. The $\Delta\delta$ values indicate that the α-conformation, in which the proton **nh1** is involved

0947-6539/01/0716-3496 $ 17.50+.50/0 *Chem. Eur. J.* **2001**, *7*, No. 16

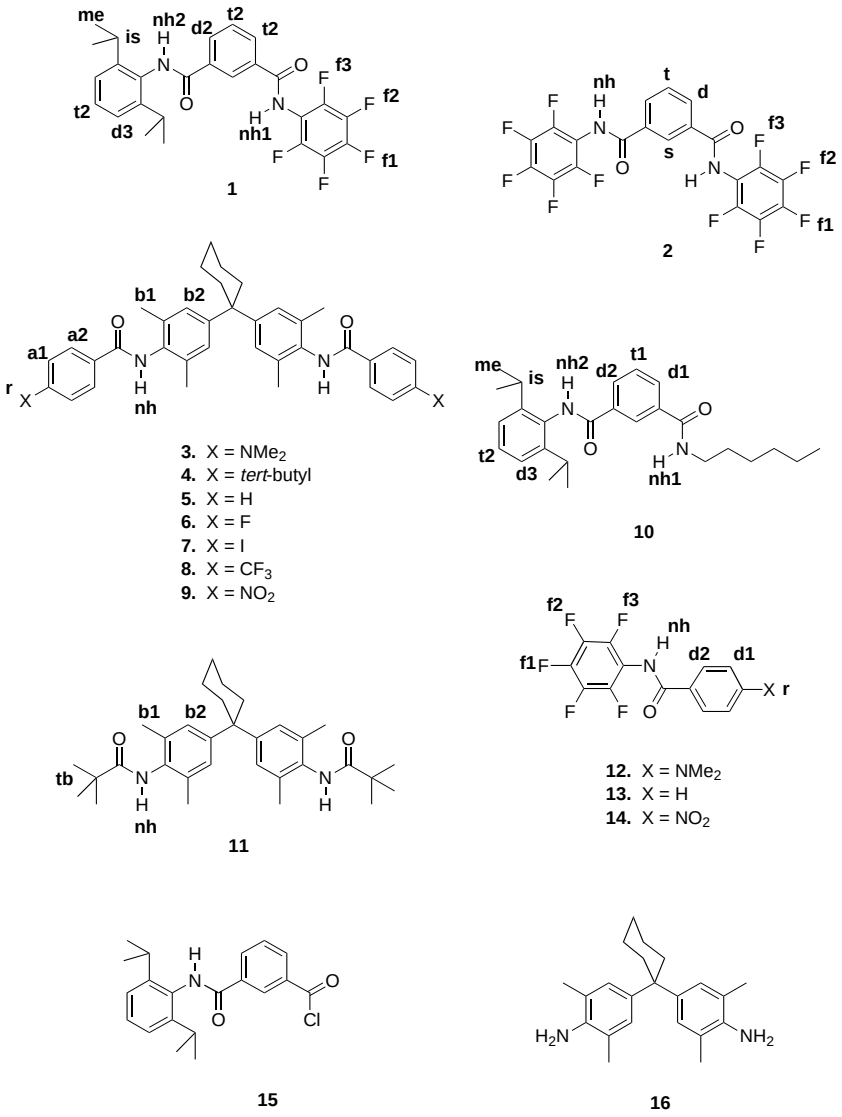

Scheme 4. Proton labelling scheme for compounds **1**–**16**.

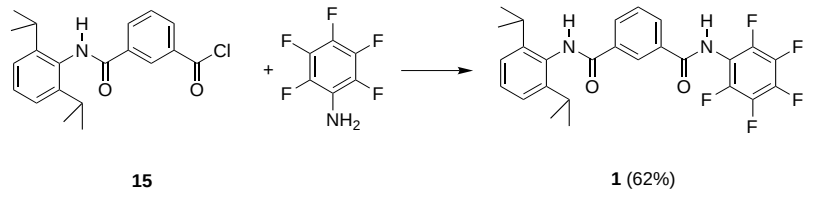

Scheme 5. Synthesis of compound **1**.

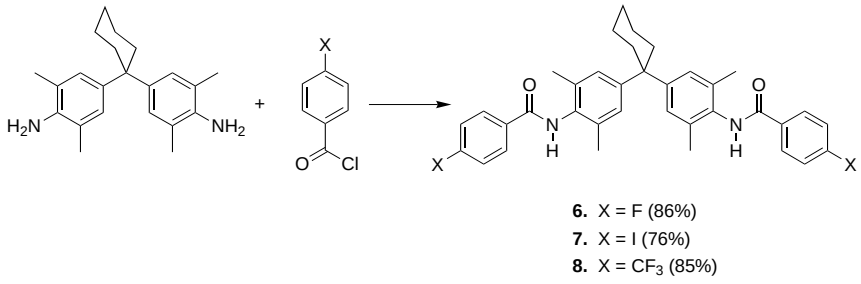

Scheme 6. Synthesis of compounds **6**–**8**.

in the H-bond, is more stable than the β-conformation, in which the proton **nh2** is H-bonded instead (Scheme 7). This is consistent with the greater acidity of **nh1**. All of the complexes show similar $\Delta\delta$ patterns for all of the protons in the central core (**t1**, **d1**, **d2**, **b1** and **b2**) (Figure 4a). Therefore, mutations do not significantly change the central structural motif in the complexes. The large upfield shifts observed for the isophthaloyl triplet (**t1**) and the two doublets (**d1** and **d2**) together with the small downfield shifts observed for **b2** indicate that the isophthaloyl rings are interacting with the bis-aniline pockets in an edge-to-face orientation. Downfield shifts for protons **a1** and **a2** in complexes **A** and **C** show that the phenyl group lies over the aniline ring. Negative $\Delta\delta$ values for the isopropyl methyl groups (**me**) show that they lie over the face of the benzoyl group. Three intermolecular NOEs were observed in a ROESY (Rotating-frame Overhauser Enhancement Spectroscopy) experiment on complex **7**·**1**, which also confirms that the isophthaloyl group is docked into the bisaniline pocket in the core of the complex and the benzoyl group lies over the 2,6-diisopropylaniline ring (Scheme 8).

In order to find out about the geometry of the pentafluorophenyl–aryl interaction in complex **A**, we needed more information. Therefore, we decided to look at the ^{19}F NMR $\Delta\delta$ values for **f1**, **f2** and **f3** in complex **A**. These values are difficult to interpret. However, they are similar when the phenyl X substituents are *tert*-butyl, H, F, I and CF_3, much larger when the substituent is NMe_2 and very small when the substituent is NO_2 (Figure 4b). This suggests some change in conformation in these systems. All of the $\Delta\delta$ values of complex **1**·

Table 1. Association constants K_a and Gibbs free energy of binding.

Complex	K_a [M^{-1}]	ΔG_{exp} [kJ mol^{-1}]
3-1	145 ± 8	– 12.2
4-1	88 ± 6	– 11.0
5-1	54 ± 5	– 9.8
6-1	83 ± 10	– 10.8
7-1	101 ± 14	– 11.3
8-1	83 ± 9	– 10.8
9-1	265 ± 33	– 13.7
3-10	17 ± 1	– 6.9
4-10	19 ± 1	– 7.2
5-10	17 ± 1	– 6.9
6-10	40 ± 4	– 9.0
7-10	40 ± 9	– 9.0
8-10	41 ± 7	– 9.1
9-10	146 ± 6	– 12.2
11-1	27 ± 2	– 8.1
11-10	6 ± 1	– 4.4

Table 3. Complexation-induced changes in ^{1}H NMR chemical shifts obtained by NMR titrations in chloroform at 295 K.[a]

	Bisaniline Compounds Δδ					
Complex	a1	a2	nh	b1	b2	r
3-1	– 0.27	– 0.15	0.48	– 0.03	0.10	– 0.04
4-1	– 0.15	– 0.28	0.68	– 0.04	0.14	– 0.04
5-1	– 0.24	– 0.16	0.81	– 0.05	0.13	– 0.11
6-1	– 0.22	– 0.10	0.78	– 0.03	0.12	–
7-1	– 0.25	– 0.11	0.50	– 0.02	– 0.13	–
8-1	– 0.33	– 0.11	1.12	– 0.04	0.17	–
9-1	– 0.12	– 0.04	0.43	– 0.01	– 0.04	–
3-10	– 0.24	– 0.12	0.84	– 0.12	0.07	– 0.05
4-10	– 0.22	– 0.08	0.93	– 0.05	0.11	– 0.04
5-10	– 0.18	– 0.04	0.43	0.15	0.16	0.00
6-10	– 0.18	– 0.08	0.64	– 0.20	0.20	–
7-10	– 0.22	– 0.10	0.50	– 0.10	0.17	–
8-10	– 0.20	– 0.18	0.52	– 0.11	0.12	–
9-10	– 0.34	– 0.04	1.50	– 0.11	0.11	–
11-1	–	–	0.52	– 0.09	0.10	nd
11-10	–	–	0.40	nd	0.08	nd

[a] nd indicates a value that was not determined.

9, in which the substituent (X) is the nitro group appear anomalous. The Δδ pattern is similar to the other **A** complexes, but the values are smaller by a factor of two (Figure 4a). Therefore, the geometry of this complex is probably different from the other **A** complexes.

The $\Delta\Delta G_{exp}$ values for the aromatic interactions were calculated using Equation (1) and the values are reported in Table 4. The pentafluorophenyl – aryl interaction is attractive only when the dimethylamino substituent is present in the aryl ring. For all the other substituents, repulsive interactions were

Table 2. Complexation-induced changes in ^{1}H NMR chemical shifts obtained by NMR titrations in chloroform at 295 K.[a]

	Isophthaloyl compounds Δδ												
Complex	t1	d1	d2	s	nh1	nh2	t2	d3	is	me	f1	f2	f3
3-1	– 1.16	– 0.31	– 0.35	– 0.02	1.74	0.90	– 0.03	– 0.04	– 0.02	– 0.11	1.04	– 2.50	– 1.81
4-1	– 1.36	– 0.38	– 0.51	– 0.01	1.82	0.88	0.02	– 0.03	– 0.05	– 0.13	0.52	– 0.86	– 1.01
5-1	– 1.27	– 0.40	– 0.46	0.01	1.77	0.98	– 0.02	– 0.02	– 0.05	– 0.14	0.39	– 1.17	– 0.96
6-1	– 1.43	– 0.46	– 0.55	– 0.02	1.48	0.66	– 0.03	– 0.03	– 0.06	– 0.15	0.31	– 0.60	– 0.67
7-1	– 1.69	– 0.45	– 0.52	– 0.03	1.39	0.53	– 0.01	– 0.01	– 0.09	– 0.13	0.29	– 0.49	– 0.23
8-1	– 1.70	– 0.43	– 0.52	– 0.02	1.44	0.62	– 0.02	– 0.02	– 0.08	– 0.15	0.22	– 0.51	– 0.68
9-1	– 0.70	– 0.17	– 0.29	0.02	0.57	0.3	0.05	0.01	– 0.04	– 0.06	0.14	0.07	– 0.21
3-10	– 0.93	– 0.32	– 0.13	0.00	0.88	1.38	– 0.03	– 0.04	0.02	– 0.11	–	–	–
4-10	– 1.48	– 0.47	– 0.21	0.01	1.01	1.43	0.02	– 0.04	– 0.03	– 0.13	–	–	–
5-10	– 1.17	– 0.48	– 0.18	– 0.01	0.79	1.32	– 0.02	– 0.05	– 0.05	– 0.17	–	–	–
6-10	– 1.03	– 0.45	– 0.19	– 0.03	0.53	1.00	0.02	– 0.02	– 0.04	– 0.12	–	–	–
7-10	– 1.60	– 0.50	– 0.26	– 0.09	0.45	0.74	0.01	– 0.01	– 0.05	– 0.12	–	–	–
8-10	– 1.78	– 0.56	– 0.65	– 0.06	0.43	1.12	– 0.01	– 0.01	– 0.06	– 0.13	–	–	–
9-10	– 1.32	– 0.41	– 0.29	0.01	0.59	0.96	– 0.06	– 0.02	– 0.07	– 0.13	–	–	–
11-1	– 1.29	– 0.56	– 0.46	nd	1.78	0.67	– 0.05	– 0.05	– 0.03	– 0.06	0.64	– 0.98	– 0.73
11-10	– 1.29	– 0.66	– 0.25	nd	0.98	1.15	– 0.07	– 0.09	– 0.03	– 0.06	–	–	–

[a] nd indicates a value that was not determined.

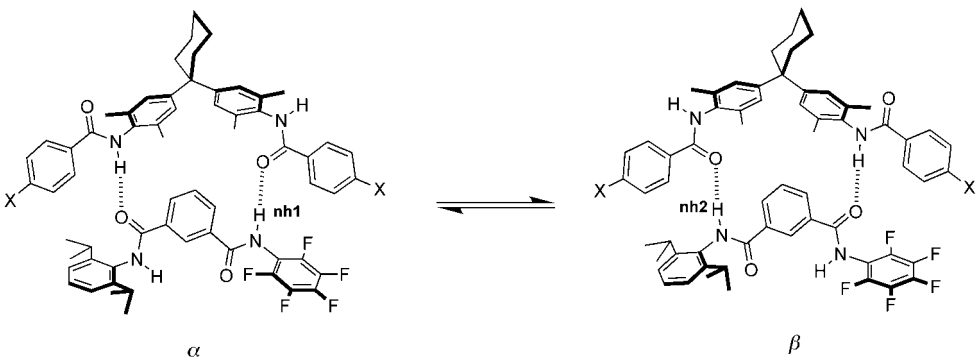

Scheme 7. Conformational equilibrium observed in complex **A**. The Δδ value for **nh1** is always bigger than the Δδ value for **nh2**. Therefore, the α-conformation is more stable than the β one (X = NMe_2, *t*Bu, H, F, I, CF_3, NO_2).

0947-6539/01/0716-3498 $ 17.50+.50/0 *Chem. Eur. J.* **2001**, *7*, No. 16

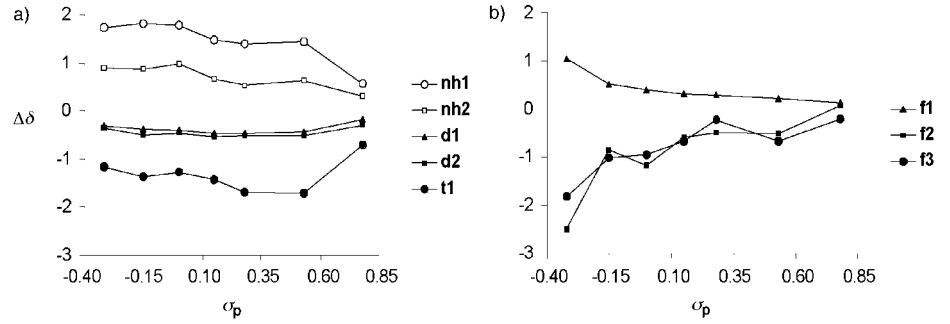

Figure 4. a) Complexation-induced changes in the chemical shift ($\Delta\delta$) for the central core protons in complex **A** plotted as a function of the Hammett substituent constant σ_p; b) Complexation-induced changes in the chemical shift for the fluorine atoms of the pentafluorophenyl group plotted as a function of the Hammett substituent constant σ_p.

observed and they increase with an increase in the electron-withdrawing character of the substituent. In order to interpret the trends in Table 4, we have plotted the $\Delta\Delta G_{exp}$ values against the Hammett substituents parameters (σ_p), which measure the electronic effects of the substituents on the aromatic ring. We have previously used this approach for simple edge-to-face aromatic interactions obtaining a straight line correlation.[7] However, it is evident from Figure 5 that the Hammett plot is bent. Bent Hammett plots are generally observed when the mechanism of a reaction changes upon altering the substituents.[22] In our case, we are looking at noncovalent interactions, and therefore the bent Hammett plot is related to a change in the mechanism of interaction. The NMR $\Delta\delta$ data suggest that the change in mechanism is a change in the geometry of the interaction. The **f1**, **f2**, and **f3** $\Delta\delta$ values, change dramatically going from complex **3·1** to complex **9·1** (Figure 4b). Indeed, the shapes of the ^{19}F NMR $\Delta\delta$ vs σ_p plots in Figure 4b are very similar to the Hammett plot in Figure 5.

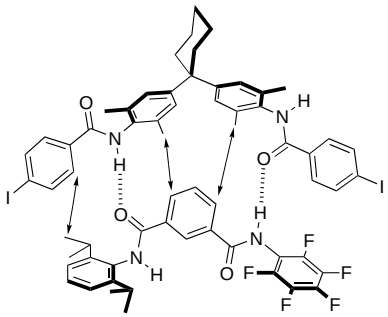

Scheme 8. Intermolecular NOEs from a ROESY experiment on an equimolar mixture of **1** and **7** in $CDCl_3$ at 295 K.

Table 4. Pentafluorophenyl–aryl interaction energies and Hammett substituent constants.

X	σ_p	Interaction energies [kJ mol^{-1}] $\Delta\Delta G_{exp}$	ΔE_{calcd} [Eqs. (4) and (5)]
NMe_2	−0.32	−1.6 ± 0.7	−3.8
*t*Bu	−0.15	0.0 ± 0.5	0.2
H	0.00	0.9 ± 0.5	0.9
F	0.15	1.9 ± 0.6	1.8
I	0.28	1.4 ± 0.6	0.9
CF_3	0.53	2.0 ± 0.6	–
NO_2	0.78	2.2 ± 0.5	3.9

Molecular mechanics calculations: Previously, we used a molecular mechanics approach and an improved version of the XED force field to predict the magnitude of the interaction energy between aromatic rings in an edge-to-face orientation.[23, 24] Here, we apply the same approach to try and gain more insight into the causes of the bent Hammett plot.

Using the double mutant cycle in Scheme 9, the values of ΔE_{calcd} for X = NH_2, *tert*-butyl,

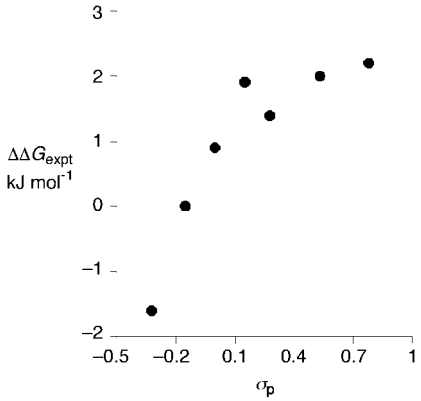

Figure 5. Aromatic interaction energies ($\Delta\Delta G_{exp}$) plotted as a function of the Hammett substituent constants (σ_p).

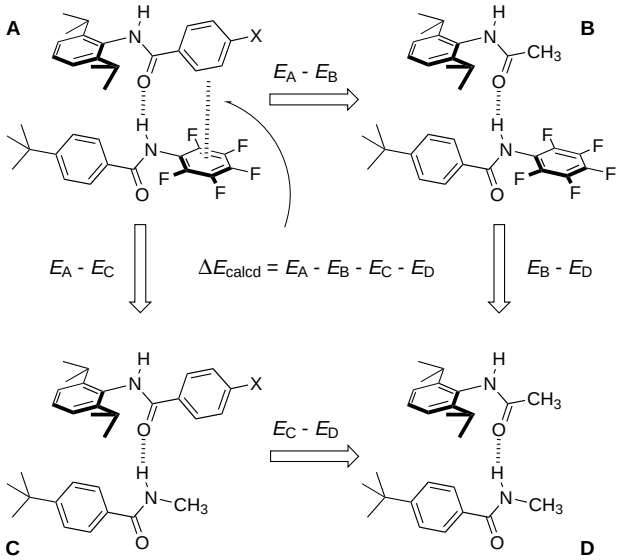

Scheme 9. Double mutant cycle (X = NH_2, *t*Bu, H, F, I, CF_3, NO_2).

H, F, I and NO_2 were calculated (the value of ΔE_{calcd} for the CF_3 substituent was not calculated because the XED force field is not yet fully parameterised for aliphatic fluorine). The truncated complexes in Scheme 3 represent the right-hand part of the experimentally studied complexes in Scheme 2 and the same key interactions are present. As demonstrated

before, it is computationally easier to deal with these smaller model complexes than the full structures in Scheme 2. The equilibrium between the α- and β-conformations (Scheme 10)

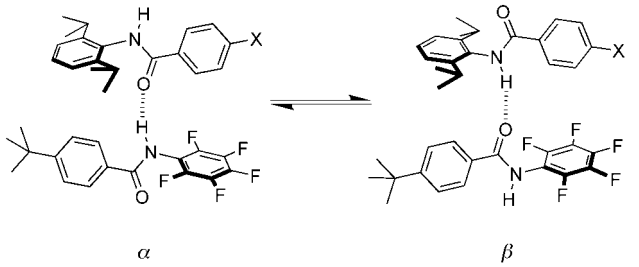

α β

Scheme 10. Conformational equilibrium in model complexes (X = NH_2, *t*Bu, H, F, I, NO_2).

was considered by minimising both structures and using the Boltzmann weighted average (E_{calcd}) of the energies of the two conformations [E_α and E_β, Eqs. (2) – (4)]. In these expressions, χ_α is the mole fraction of complex α at equilibrium.

$$E_{calcd} = \chi_\alpha E_\alpha + (1 - \chi_\alpha) E_\beta \quad (2)$$

$$1/\chi_\alpha = 1 + \exp\{(E_\alpha - E_\beta)/RT\} \quad (3)$$

$$\Delta E_{calcd} = E_A - E_B - E_C + E_D \quad (4)$$

All of the complexes in Scheme 9 were constructed using the X-ray crystal structure of the dimer **17** (Figure 2a) and optimised as explained in the Experimental Section. In other words, the starting point for complex **A** was an edge-to-face geometry between the aryl and pentafluorophenyl rings. Calculations were performed in a vacuum using a dielectric constant of two. We have previously found that if the values of ΔE_{calcd} [Eq. (5)] are divided by a factor of 2.2, the results are in good agreement with our experimental data and this factor represents in some way the dielectric effect of $CHCl_3$ desolvation.

$$\Delta E_{calcd} = 2.2 \Delta\Delta G_{exp} \quad (5)$$

Equations (2), (3) and (4) were used to calculate the chemical double mutant cycle energies for the six substituents (NH_2, *tert*-butyl, H, F, I and NO_2) and then Equation (5) was used to predict the interaction energies in Table 4.

After energy minimisation, **A** complexes with the phenyl substituent X = *tert*-butyl, H, F, I and NO_2 retained the initial edge-to-face geometry with RMS (Root Mean Square) differences of 0.2 and 0.3 Å between the minimised complexes and the starting structures (Figure 6a). In contrast, when X = NH_2, complex **A** changed conformation in order to allow the aryl ring to stack with the pentafluorophenyl ring (Figure 6b), as observed in the X-ray crystal structures for this substituent. The value of ΔE_{calcd} for this interaction does not correlate well with the corresponding experimental value (Figure 7) and this may reflect some difference in the desolvation energy as a consequence of the conformational change required to produce the stacking interaction. For all the other substituents, the calculated and experimental values agree well:

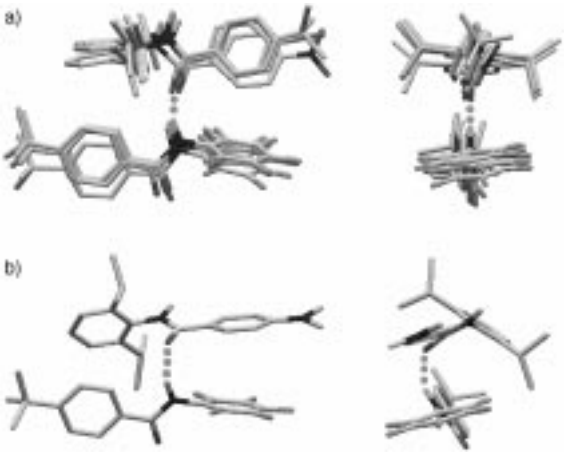

Figure 6. a) Two views of an overlay between minimised **A** complexes with X = *tert*-butyl, H, F, I and NO_2; b) Two views of the minimised structure of complex **A** when X = NH_2.

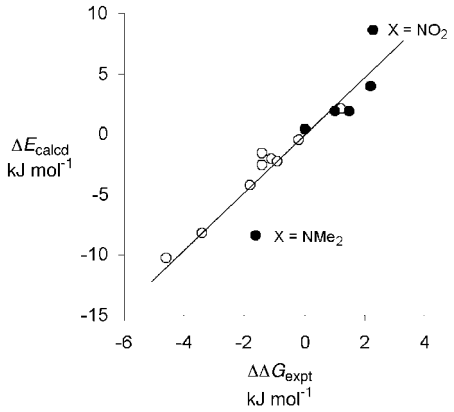

Figure 7. Correlation between the experimental measurements and the calculated energies using the XED force field. ○: previously calculated data on the simple edge-to-face interaction.[24] ●: pentafluorophenyl – aryl interactions discussed here. The outliers (X = NO_2 and NMe_2) are discussed in the text.

Figure 7 shows this data along with the previously calculated data for simple edge-to-face aromatic interactions.[24]

The calculated structures show that the interaction energies measured experimentally correspond to edge-to-face interactions between the edge of the aryl ring and the face of the pentafluorophenyl ring except when X = NMe_2. In the edge-to-face geometry, the positive protons on the aryl ring are sitting over the positive charge on the face of the pentafluorophenyl ring (Figure 8a). This creates an electrostatic repul-

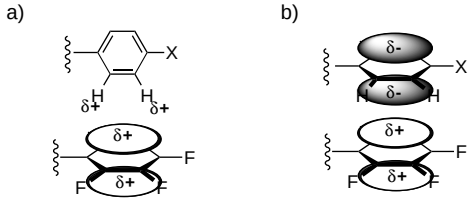

Figure 8. Representation of the charge distribution of the pentafluorophenyl – aryl edge-to-face interaction (a) and the pentafluorophenyl – aryl stacking interaction (b) (X = NMe_2, *t*Bu, H, F, I, CF_3, NO_2).

0947-6539/01/0716-3500 $ 17.50+.50/0 *Chem. Eur. J.* **2001**, *7*, No. 16

sion between the rings, which grows when the magnitude of the positive charge on the phenyl protons increases as a result of electron-withdrawing substituents. There appears to be a limit to the repulsion tolerated before a change in the structure of the complex takes place ($+2\ kJ\,mol^{-1}$). When $X = NO_2$ the calculated repulsion between the pentafluorophenyl and the aryl ring is $+3.9\ kJ\,mol^{-1}$, but the experimental value is $+2.2\ kJ\,mol^{-1}$. Although the pattern of $\Delta\delta$ values for this complex is similar to the others, the magnitudes of the values are lower, which may reflect conformational rearrangement to reduce the repulsive interaction.

The electron-donating effect of the NMe_2 substituent increases the negative charge on the face of the aryl ring and this leads to a strong driving force for the aryl ring to stack with the pentafluorophenyl ring. In this geometry, the negative aromatic cloud of the aryl ring interacts with the partial positive charge on the pentafluorophenyl ring which results in the only attractive interaction observed in this system (Figure 8b).

Conclusion

We have used the double mutant cycle approach to investigate the pentafluorophenyl–aryl interaction. From the values of $\Delta\Delta G_{exp}$, it is clear that the interaction is repulsive except for the NMe_2 substituted aryl group, which shows an attractive interaction. These results are generally consistent with an edge-to-face geometry between the aryl group and the pentafluorophenyl ring in complex **A** (Scheme 2). In this geometry, the positive charges on the protons of the aromatic ring interact with the partial positive charge located at the centre of the pentafluorophenyl ring. The Hammett plot shows that there is a change in the nature of the interaction when electron-withdrawing substituents are replaced with electron-donating substituents. The NMR chemical shift analysis, X-ray crystal structures and molecular mechanics calculations show that the change in the interaction from repulsive to attractive is associated with a change in the structure of complex **A**. When $X = NMe_2$ there is a strong driving force for stacking, whereas the other systems remain edge-to-face. The XED force field was used to predict the experimental results and the calculated pentafluorophenyl–aryl interaction agrees with the experimental data.

Experimental Section

Computer modelling: All the calculations were run on a Silicon Graphics Indigo2 workstation using the XED force field with a dielectric constant of 2.[23] The following XED charge distribution for the fluorine atom type allowed us to reproduce a hexafluorobenzene quadrupole: $31_{distance} = 0.37$; $32_{distance} = 0.45$; $33_{distance} = 0.00$; $34_{distance} = 0.30$; $35_{distance} = 0.71$; $31_{charge} = 1.00$; $32_{charge} = 1.00$; $33_{charge} = 0.00$; $34_{charge} = 1.50$; $35_{charge} = 0.50$ (see Figure 9).

The model complexes used for the calculations were constructed starting from the X-ray crystal structure of the dimer of **17** (Figure 2a). **A** complexes in the α-conformation were constructed by substitution of the *para*-*tert*-butyl group in the aromatic ring **a** with the appropriate substituent and the protons and the two isopropyl groups of the aromatic ring **d** were replaced by fluorine atoms. The same substitutions were performed in aromatic ring **c** and **b**, for the construction of **A** complexes in the β-conformation. **B** complexes in the α- and β-conformations were constructed by replacing aromatic rings **a** or **c** with methyl groups respectively and by replacing the protons and the isopropyl groups in the rings **b** or **d** with fluorine atoms. **C** complexes in the α- and β-conformations were constructed by replacing the aromatic rings **d** and **b** with methyl groups respectively and replacing the *tert*-butyl groups in the aromatic rings **a** or **c** with the appropriate substituents. Finally, the **D** complexes were obtained by substitution of aromatic rings **a** and **d** with methyl groups for the α-conformer and **b** and **c** for the β-conformer. The complexes were subjected to energy minimisation using a maximum number of iterations of 8000, which guaranteed complete minimisation.

NMR binding experiments: A Bruker AC250 NMR spectrometer was used for all of the ^1H and ^{19}F NMR titrations. Each titration was carried out by preparing a solution of the host (3 mL) at known concentration ($\approx 10^{-3}$ M) in $CDCl_3$. A sample (0.5 mL) was placed in a NMR tube. A solution of guest (2 mL) at known concentration ($\approx 10^{-2}$ M) was prepared using the solution of host as solvent, so that the concentration of host remained constant during the titration. The ^1H NMR spectrum of the host solution was recorded and the same operation was repeated after each subsequent addition of aliquots of the guest solution into the NMR tube containing the host solution. The *NMRTit HG* fit program was used to analyse changes in chemical shifts during the titration to obtain the binding constant and the values of limiting complexation-induced changes in chemical shift for the protons of the host and the guest.

General procedures: Chemicals were purchased and used without further purification. CH_2Cl_2 was dried by distillation from CaH. TLC was carried out using 0.2 mm Kieselgel $60\,F_{254}$ precoated aluminium sheets, commercially available from Merck. Visualisation was done by fluorescence quenching at 254 nm, or by exposure to a solution of ninhydrin (5%) in ethanol followed by heating at 200 °C for 15 s. Flash column chromatography was carried out using "flash" Kieselgel 60 (230–400 mesh) purchased from Merck.

^1H, ^{13}C and ^{19}F spectra were recorded on either a Bruker AC250 or AMX400 spectrometer. All chemical shifts are quoted on the δ scale and the coupling constants are expressed in Hz.

Preparation of *N*-pentafluorophenyl-*N*′-[(2,6-diisopropyl)phenyl]isophthalamide (1): Compound 3-{*N*-[(2,6-diisopropyl)phenyl]formamido}-benzoyl chloride (0.50 g, 1.45 mmol) was added portionwise to a stirred solution of pentafluoroaniline (0.29 g, 1.6 mmol) in CH_2Cl_2 (10 mL) over a 5 min period. Following the addition, the mixture was stirred at room temperature for four days before dilution with $CHCl_3$ (40 mL). The organic solution was concentrated in vacuo and the crude product recrystallised from $CHCl_3$ to give the title compound (0.44 g, 62% yield) as a white solid. M.p. > 250 °C.

^1H NMR (250 MHz, $CDCl_3$, 25 °C, TMS): $\delta = 8.71$ (s, 1H; **s**), 8.16 (m, 1H; **d1**), 8.11 (m, 1H; **d2**), 7.72 (s, 1H; **nh1**), 7.69 (t, $J = 7.9$ Hz, 1H; **t1**), 7.44 (s, 1H; **nh2**), 7.36–7.41 (m, 1H; **t2**), 7.24 (m, 2H; **d3**), 3.12 (sep, $J = 6.8$ Hz, 2H; **is**), 1.24 (d, $J = 6.9$ Hz, 12H; **me**); ^{13}C NMR (63 MHz, $[D_6]$DMSO, 25 °C): $\delta = 23.78, 24.05, 28.67, 123.47, 127.92, 128.24, 129.52, 131.32, 131.64, 132.99, 133.29, 135.28, 146.58, 165.57, 165.93$; ^{19}F NMR (235 MHz, $CDCl_3$, 25 °C): $\delta = -144.79$ (d, $J = 14.1$ Hz, 2F; **f3**), -156.24 (t, $J = 14.0$ Hz, 1F; **f1**),

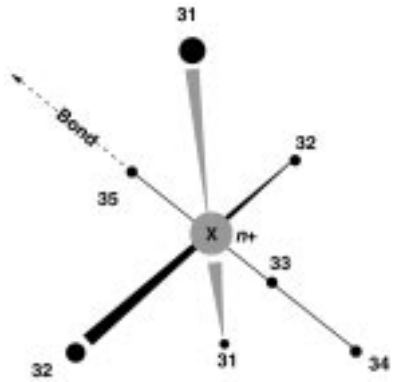

Figure 9. XED orbital descriptor.

−162.13 to −162.28 (m, 2F; **f2**); MS (FAB+): *m/z*: 491 $[M+H]^+$; elemental analysis calcd (%) for $C_{26}H_{23}F_5N_2O_2$ (490): C 63.67, H 4.73, N 5.71; found C 63.62, H 4.74, N 5.40.

Preparation of *N,N′*-bis-pentafluorophenyl isophthalamide (2): Isophthaloyl dichloride (0.30 g, 1.5 mmol) was added in one portion to a stirred solution of pentafluoroaniline (1.08 g, 5.9 mmol) in dry CH_2Cl_2 at room temperature. Following the addition, the mixture was stirred at room temperature for six days, whereupon a white precipitate was produced. The crude reaction mixture was diluted with $CHCl_3$ (50 mL) and the organic layer washed successively with NaOH (1M, 30 mL), HCl (1M, 30 mL) and water (2 × 50 mL) before it was dried (Na_2SO_4), filtered and concentrated in vacuo. Recrystallisation from EtOH/water gave the pure title compound (0.59% yield) as a white solid. M.p. > 260 °C.

^{1}H NMR (250 MHz, [D$_6$]DMSO, 25 °C, TMS): $\delta = 10.83$ (s, 1H), 8.63 (s, 1H), 8.26 (d, $J = 7.6$ Hz, 2H), 7.77 (t, $J = 7.5$ Hz, 1H); ^{19}F NMR (235 MHz, $CD_3OD/CDCl_3$, 25 °C): $\delta = -145.19$ (d, $J = 23.2$ Hz, 4F; **f3**), −156.70 (t, $J = 23.2$ Hz, 2F; **f1**), −162.30 to −162.70 (m, 4F; **f2**); MS (FAB): *m/z*: 497 $[M+H]^+$; elemental analysis calcd (%) for $C_{20}H_6F_{10}N_2O_2$ (496): C 48.41, H 1.22, N 5.64; found C 48.64, H 1.25, N 5.57.

General procedure for the synthesis of compounds 6–8: A solution of 4-substituted benzoyl chloride (3.8 mmol) in dry CH_2Cl_2 (30 mL) was added dropwise over 20 min to a stirred solution of bisaniline **16** (0.6 g, 1.2 mmol) and triethylamine (0.5 mL, 4 mmol) in dry CH_2Cl_2 (12 mL). Following the addition, the mixture was stirred at room temperature for 12 h. The crude reaction mixture was diluted with CH_2Cl_2 (30 mL) and the organic layer washed successively with NaOH (1M, 30 mL), HCl (1M, 30 mL) and water (2 × 30 mL) before it was dried (Na_2SO_4), filtered and concentrated in vacuo. Purification by recrystallisation gave the pure compounds.

***N,N′*-(4-Difluorobenzoyl)-{1,1-bis[(4-amido-3,5-dimethyl)phenyl]cyclohexane} (6)**: Compound **6** was prepared following the general procedure described above using 4-fluorobenzoyl chloride (0.45 mL). The crude product was recrystallised from $CHCl_3$/petroleum ether to yield a white solid (0.580 g, 86%). M.p. 178–180 °C.

^{1}H NMR (250 MHz, $CDCl_3$, 25 °C, TMS): $\delta = 7.87-7.81$ (m, 4H; **a2**), 7.43 (s, 2H; **nh**), 7.14–7.05 (m, 4H; **a1**), 7.01 (s, 4H; **b2**), 2.23 (s, 12H; **b1**); ^{13}C NMR (63 MHz, [D$_6$]DMSO, 25 °C): $\delta = 18.63$, 22.89, 26.31, 37.02, 45.39, 115.24, 115.62, 126.94, 129.67, 129.81, 130.50, 131.38, 135.09, 147.63, 162.76, 165.04, 166.76; MS (FAB+): *m/z*: 567 $[M]^+$; elemental analysis calcd (%) for $C_{36}H_{36}F_2N_2O_2$ (567): C 76.29, H 6.40, N 4.94; found C 76.45, H 6.46, N 4.84.

***N,N′*-(4-Diiodoobenzoyl)-{1,1-bis[(4-amido-3,5-dimethyl)phenyl]cyclohexane} (7)**: Compound **7** was prepared following the general procedure described above using 4-iodobenzoyl chloride (1.010 g). The crude product was recrystallised from $CHCl_3$/petroleum ether to yield a white solid (0.680 g, 73%). M.p. 210–214 °C.

^{1}H NMR (250 MHz, $CDCl_3$, 25 °C, TMS): $\delta = 7.75$ (d, $J = 8.2$ Hz, 4H; **a2**), 7.64 (s, 2H; **nh**), 7.50 (d, $J = 8.2$ Hz, 4H; **a1**), 6.94 (s, 4H; **b2**), 2.06 (s, 12H; **b1**); ^{13}C NMR (63 MHz, [D$_6$]DMSO, 25 °C): $\delta = 18.86$, 22.88, 37.05, 45.42, 98.70, 127.10, 128.82, 130.98, 133.93, 134.90, 137.92, 147.61, 165.16; MS (FAB+): *m/z*: 783 $[M]^+$; elemental analysis calcd (%) for $C_{36}H_{36}I_2N_2O_2$ (783): C 55.26, H 4.66, N 3.58, I 32.44; found C 55.11, H 4.66, N 3.40, I 32.68.

***N,N′*-(4-Di-trifluoromethylbenzoyl)-{1,1-bis[(4-amido-3,5-dimethyl)phenyl]cyclohexane} (8)**: Compound **8** was prepared following the general procedure described above using 4-trifluoromethylbenzoyl chloride (0.790 g). The crude product was recrystallised from $CHCl_3$/petroleum ether to yield a white solid (0.680 g, 85%). M.p. 205–207 °C.

^{1}H NMR (250 MHz, $CDCl_3$, 25 °C, TMS): $\delta = 7.94$ (d, $J = 7.9$ Hz, 4H; **a2**), 7.71 (d, $J = 8.2$ Hz, 4H; **a1**), 7.53 (s, 2H; **nh**), 7.00 (s, 4H; **b2**), 2.16 (s, 12H; **b1**); ^{13}C NMR (63 MHz, $CDCl_3$, 25 °C): $\delta = 18.82$, 22.88, 26.28, 37.02, 45.43, 125.74, 127.14, 127.69, 130.84, 134.91, 137.83, 147.78, 164.71; MS (FAB+): *m/z*: 667 $[M]^+$; elemental analysis calcd (%) for $C_{38}H_{36}F_6N_2O_2 + H_2O$ (685): C 66.66, H 5.59, N 4.09; found C 67.48, H 5.59, N 4.09.

General procedure for the synthesis of compounds 12–14: The compound 4-substituted benzoyl chloride (6.0 mmol) was added in a dropwise fashion to a stirred solution of pentafluoroaniline (0.75 g, 4.1 mmol) in CH_2Cl_2 (12 mL) over a 10 min period. Following the addition, the mixture was stirred at room temperature for 20 h before dilution with $CHCl_3$ (35 mL) and washing with water (2 × 30 mL). The organic solution was dried (Na_2SO_4) and the solvent was removed in vacuo. The crude product was recrystallised to give the pure product.

***N*-Pentafluorophenyl-4-dimethylamino-benzamide (12)**: Compound **12** was prepared following the general procedure described above using 4-dimethylaminobenzoyl chloride (1.100 g). The crude product was recrystallised from $CHCl_3$/petroleum ether to yield a white solid (0.880 g, 65%). M.p. 244–245 °C.

^{1}H NMR (250 MHz, $CDCl_3$, 25 °C, TMS): $\delta = 7.80$ (d, $J = 8.9$ Hz, 2H; **a2**), 7.18 (s, 1H; **nh**), 6.70 (d, $J = 9.2$ Hz, 2H; **a1**), 3.06 (s, 6H; **r**); ^{13}C NMR (63 MHz, [D$_6$]DMSO, 25 °C): $\delta = 40.14$, 111.29, 118.87, 130.02, 153.36, 165.47; ^{19}F NMR (235 MHz, [D$_6$]DMSO, 25 °C): $\delta = -145.01$ (d, $J = 17.4$ Hz, 2F; **f3**), −157.84 (t, $J = 21.9$ Hz, 1F; **f1**), −163.26 to −163.50 (m, 2F; **f2**); MS (FAB+): *m/z*: 331 $[M+H]^+$; elemental analysis calcd (%) for $C_{15}H_{11}F_5N_2O + H_2O$ (348): C 51.73, H 3.76, N 8.04; found C 51.74, H 3.70, N 8.14.

Crystal data for $C_{15}H_{11}F_5N_2O$: $M_r = 330.26$, crystallises from acetone/water as white blocks; crystal dimensions 0.40 × 0.40 × 0.20 mm. Monoclinic, $a = 7.1585(10)$, $b = 23.551(3)$, $c = 8.6829(12)$ Å, $\beta = 112.667(3)°$, $U = 1350.8(3)$ Å^3, $Z = 4$, $\rho = 1.624$ mg m^{-3}, space group $P2_1/n$ (a nonstandard setting of $P2_1/cC_2^5$ *h′* No. 14), $Mo_{K\alpha}$ radiation ($\bar{\lambda} = 0.71073$ Å), $\mu(Mo_{K\alpha}) = 0.151$ mm^{-1}, $F(000) = 672$.

Crystallographic data (excluding structure factors) for the structure reported in this paper have been deposited with the Cambridge Crystallographic Data Centre as supplementary publication no. CCDC-153096. Copies of the data can be obtained free of charge on application to CCDC, 12 Union Road, Cambridge CB21EZ, UK (fax: (+44) 1223-336-033; e-mail: deposit@ccdc.cam.ac.uk).

***N*-Pentafluorophenyl-benzamide (13)**: Compound **13** was prepared following the general procedure described above using benzoyl chloride (0.840 g). The crude product was recrystallised from $CHCl_3$/petroleum ether to yield a white solid (0.820 g, 69%). M.p. 183–185 °C.

^{1}H NMR (250 MHz, $CDCl_3$, 25 °C, TMS): $\delta = 7.95-7.89$ (m, 2H; **a2**), 7.66–7.59 (m, 1H; **r**), 7.56–7.48 (m, 2H; **a1**), 7.47 (s, 1H; **nh**); ^{13}C NMR (63 MHz, [D$_6$]DMSO, 25 °C): $\delta = 128.42$, 129.18, 133.07, 133.66; ^{19}F NMR (235 MHz, [D$_6$]DMSO, 25 °C): $\delta = -144.80$ (m, 2F; **f3**), −156.90 (t, $J = 24.0$ Hz, 1F; **f1**), −162.86 to −163.05 (m, 2F; **f2**); MS (FAB+): *m/z*: 288 $[M+H]^+$; elemental analysis calcd (%) for $C_{13}H_6F_5NO + H_2O$ (305): C 51.16, H 2.64, N 4.59; found C 51.36, H 2.54, N 4.53.

Crystal data for $C_{13}H_6F_5NO$: $M_r = 287.19$, crystallised from dichloromethane/petroleum ether as white plates; crystal dimensions 0.35 × 0.20 × 0.10 mm. Triclinic, $a = 4.8309(17)$, $b = 9.826(5)$, $c = 24.501(10)$ Å, $\alpha = 89.98(3)°$, $\beta = 84.98(4)°$, $\gamma = 89.11(3)°$, $U = 1158.4(8)$ Å^3, $Z = 4$, $\rho = 1.647$ mg m^{-3}, space group $P\bar{1}$, (C_i^1, No. 2) $Mo_{K\alpha}$ radiation ($\bar{\lambda} = 0.71073$ Å), $\mu(Mo_{K\alpha}) = 0.160$ mm^{-1}, $F(000) = 576$.

Crystallographic data (excluding structure factors) for the structure reported in this paper have been deposited with the Cambridge Crystallographic Data Centre as supplementary publication no. CCDC-153098. Copies of the data can be obtained free of charge on application to CCDC, 12 Union Road, Cambridge CB21EZ, UK (fax: (+44) 1223-336-033; e-mail: deposit@ccdc.cam.ac.uk).

***N*-Pentafluorophenyl-4-nitro-benzamide (14)**: Compound **14** was prepared following the general procedure described above using 4-nitrobenzoyl chloride (1.110 g). The crude product was crystallised with $CHCl_3$ to yield a white solid (1.080 g, 78%). M.p. 155–156 °C.

^{1}H NMR (250 MHz, $CDCl_3$, 25 °C, TMS): $\delta = 8.28$ (d, $J = 8.3$ Hz, 2H; **a2**), 7.31 (d, $J = 8.3$ Hz, 2H; **a1**), 7.49 (s, 1H; **nh**); ^{13}C NMR (63 MHz, [D$_6$]DMSO, 25 °C): $\delta = 124.36$, 130.02, 138.28, 150.23, 164.48; ^{19}F NMR (235 MHz, [D$_6$]DMSO, 25 °C): $\delta = -144.77$ (d, $J = 17.4$ Hz, 2F; **f3**), −156.33 (t, $J = 21.9$ Hz, 1F; **f1**), −162.60 to −162.75 (m, 2F; **f2**); MS (EI): *m/z*: 332 $[M]^+$; elemental analysis calcd (%) for $C_{13}H_5F_5N_2O_3 + H_2O$ (350): C 44.59, H 2.01, N 8.00; found C 44.63, H 2.06, N 8.10.

Crystal data for $C_{13}H_5F_5N_2O_3$: $M_r = 332.19$, crystallised from $CHCl_3$ as white needles; crystal dimensions 0.35 × 0.07 × 0.07 mm. Monoclinic, $a = 5.000(6)$, $b = 24.28(3)$, $c = 20.52(3)$ Å, $\beta = 94.41(9)°$, $U = 2483(5)$ Å^3, $Z = 8$, $\rho = 1.777$ mg m^{-3}, space group Cc, $Mo_{K\alpha}$ radiation ($\bar{\lambda} = 0.71073$ Å), $\mu(Mo_{K\alpha}) = 0.176$ mm^{-1}, $F(000) = 1328$.

Crystallographic data (excluding structure factors) for the structure reported in this paper have been deposited with the Cambridge Crystallographic Data Centre as supplementary publication no. CCDC-153097.

0947-6539/01/0716-3502 $ 17.50+.50/0 *Chem. Eur. J.* **2001**, *7*, No. 16

Copies of the data can be obtained free of charge on application to CCDC, 12 Union Road, Cambridge CB21EZ, UK (fax: (+44)1223-336-033; e-mail: deposit@ccdc.cam.ac.uk).

Acknowledgements

We thank the EPSRC (J.M.S), the BBSRC (G.C.), the Spanish government (J.L.J.B.) and the Lister Institute (C.A.H.) for funding.

[1] C. A. Hunter, *J. Mol. Biol.* **1993**, *230*, 1025.
[2] C. A. Hunter, J. Singh, J. M. Thornton, *J. Mol. Biol.* **1991**, *218*, 837.
[3] K. A. Dill, *Biochemistry* **1990**, *29*, 7133.
[4] L. Serrano, M. Bycroft, A. R. Fersht, *J. Mol. Biol.* **1991**, *218*, 465.
[5] F. Cozzi, M. Cinquini, R. Annunziata, T. Dwyer, J. S. Siegel, *J. Am. Chem. Soc.* **1992**, *114*, 5729.
[6] F. Cozzi, M. Cinquini, R. Annuziata, J. S. Siegel, *J. Am. Chem. Soc.* **1993**, *115*, 5330.
[7] F. J. Carver, C. A. Hunter, E. M. Seward, *Chem. Commun.* **1998**, 775.
[8] C. A. Hunter, J. K. M. Sanders, *J. Am. Chem. Soc.* **1990**, *112*, 5525.
[9] M. Luhmer, K. Bartik, A. Dejaegere, P. Bovy, J. Reisse, *Bull. Soc. Chim. Fr.* **1994**, *131*, 603.
[10] M. R. Battaglia, A. D. Buckingham, J. H. Williams, *Chem. Phys. Lett.* **1981**, *78*, 420.
[11] C. R. Patrick, G. S. Prosser, *Nature* **1960**, *187*, 1021.
[12] J. H. Williams, J. K. Cockcroft, A. N. Fitch, *Angew. Chem.* **1992**, *104*, 1666; *Angew. Chem. Int. Ed. Engl.* **1992**, *12*, 1655.
[13] J. Vrbancich, G. L. D. Ritchie, *J. Chem. Soc. Faraday Trans. 2* **1980**, *76*, 648.
[14] F. Cozzi, F. Ponzini, R. Annunziata, M. Cinquini, J. S. Siegel, *Angew. Chem.* **1995**, *107*, 1092; *Angew. Chem. Int. Ed. Engl.* **1995**, *34*, 1019.
[15] C. A. Hunter, X. J. Lu, G. M. Kapteijn, G. van Koten, *J. Chem. Soc. Faraday Trans. 2* **1995**, *91*, 2009.
[16] G. W. Coates, A. R. Dunn, L. M. Henling, D. A. Dougherty, R. H. Grubbs, *Angew. Chem.* **1997**, *109*, 290; *Angew. Chem. Int. Ed. Engl.* **1997**, *36*, 248.
[17] G. W. Coates, A. R. Dunn, L. M. Henling, J. W. Ziller, E. B. Lobkovsky, R. H. Grubbs, *J. Am. Chem. Soc.* **1998**, *120*, 3641.
[18] H. Adams, F. J. Carver, C. A. Hunter, J. C. Morales, E. M. Seward, *Angew. Chem.* **1996**, *108*, 1628; *Angew. Chem. Int. Ed. Engl.* **1996**, *35*, 1542.
[19] H. Adams, P. L. Bernad, Jr., D. S. Eggleston, R. C. Haltiwanger, K. D. M. Harris, G. A. Hembury, C. A. Hunter, D. J. Livingstone, B. M. Kariuki, J. F. McCabe, *Chem. Commun.*, in press.
[20] A. P. Bisson, F. J. Carver, D. S. Eggleston, R. C. Haltiwanger, C. A. Hunter, D. L. Livingstone, J. F. McCabe, C. Rotger, A. E. Rowan, *J. Am. Chem. Soc.* **2000**, *122*, 8856.
[21] F. J. Carver, C. A. Hunter, D. J. Livingstone, J. F. McCabe, E. M. Seward, unpublished results.
[22] N. S. Isaccs, *Physical Organic Chemistry*, Longman, London, **1995**.
[23] J. G. Vinter, *J. Comput.-Aided Mol. Des.* **1994**, *8*, 653.
[24] G. Chessari, C. A. Hunter, C. M. R. Low, M. J. Packer, J. Vinter, C. Zonta, unpublished results.

Received: December 4, 2000 [F2909]